In the course of the explosive experiments with EMG, it was established that the displacement of the loops leads to the appearance of electrical breakdown in the working volume of the EMG and lowers the magnitude of the final current. Electrical breakdown was eliminated by decreasing the axial displacement of the loops by lowering the magnitude of the initial current and decreasing its rise time and by insulating the loops. The adopted measures made it possible to increase the magnitude of the final current in the structure studied from 0.8 to 1.4 MA, i.e., by a factor of 1.7.

LITERATURE CITED

1. J. W. Shearer, F. F. Abraham, et. al., "Explosive-driven magnetic-field compression generators," Appl. Phys., 39, No. 4 (1968).
2. G. Knopfel', Ultrastrong Pulsed Magnetic Fields [Russian translation], Mir, Moscow (1972).
3. V. K. Chernyshev, E. I. Zharinov, V. A. Demidov, and S. A. Kazakov, "High-inductance explosive magnetic generators with high energy multiplication," in: Megagauss Physics and Technology, P. I. Turchi (ed.), Plenum Press, New York (1979).
4. A. I. Pavlovskii, R. Z. Lyudaev, et al., "Formation and transmission of magnetic cumulation generators electromagnetic energy pulses," in: Megagauss Physics and Technology, P. I. Turchi (ed.), Plenum Press, New York (1979).
5. I. E. Tamm, Foundations of the Theory of Electricity [in Russian], Nauka, Moscow (1966).

INTERACTION BETWEEN A NONUNIFORMLY HEATED DIELECTRIC AND A MICROWAVE FIELD

A. G. Merzhanov, V. A. Raduchev, and É. N. Rumanov

UDC 537.226:536.421+536.46

By using the abrupt growth of electrical conductivity with temperature, the authors of [1] accomplished the melting of a dielectric due to heat transfer to the solid phase from the melt absorbing hf power. The thermal regime of interphasal boundary motion during direct current heating of a melt and during induction heating was examined in [2]. In this paper, the structure of the heat wave is investigated, which is formed in the neighborhood of the melt during microwave heating. The thermal flux and field distribution is studied, and the limit values are determined for the parameter for which the thermal stability of the melt domain still holds.

1. If a melt section is produced in a waveguide with a dielectric filler* and power is fed from a microwave generator, then the melt will be heated by absorbing this power, will heat adjacent layers of the solid phase, and melt them. Therefore, the melt domain is propagated along the waveguide toward the generator. Because of secondary heat losses, this domain will be bounded. Motion of the melt boundary along the waveguide recalls propagation of a gaseous microwave discharge investigated in [3]. A problem of the light combustion wave in a solid dielectric, which is similar in formulation, was examined in [4]. However, the presence of a phase transition (accompanied by a jump in conductivity) results in a front structure and regularities of its propagation that differ from [3, 4], as will be shown.

Heating of the solid phase of the dielectric occurs because of the intrinsic absorption of microwave power as well as because of heat influx from the melt. The main part of the heat is liberated near the melt (at temperatures close to the melting point). Therefore, it can be considered that an "intrinsic" heat liberation source acts in a certain solid phase layer adjacent to the melt. The density of the power being liberated in the solid phase is small compared with the density of the power being liberated in the melt. However, it is generally impossible to neglect it since the ratio between the widths of the heat liberation domains in the solid and liquid phases is unknown in advance. It should be determined from

*For sufficient dielectric permittivity of the substance simply a rod can be considered that will be a dielectric waveguide.

Chernogolovka. Translated from Zhurnal Prikladnoi Mekhaniki i Tekhnicheskoi Fiziki, No. 1, pp. 7-13, January-February, 1985. Original article submitted December 2, 1983.

0021-8944/85/2601-0005$09.50

the solution of the problem together with the velocity of the melting wave. The total heat liberation power in the solid dielectric can here be a quantity that is not small compared with the total power being liberated in the melt.

Depending on the microwave generator power, thermal wave propagation over a waveguide can occur in different regimes. For a sufficient magnitude of the delivered power a part of the heat liberated in the melt will go directly into melting the substance, and a part into heating the solid phase. The width of the heated solid phase layer is inversely proportional to the wave velocity and depends on the power absorbed by the dielectric. This latter is determined by the electromagnetic field distribution which depends, in turn, on the width of the heated layer. Therefore, an inverse relation holds between the electromagnetic and the thermal processes. As the microwave generator power diminishes below a certain critical value, the melt freezes, and a thermal wave similar to that considered in [3] propagates over the solid dielectric. That the heat flux from the melt becomes zero in the solid phase corresponds to the condition of a change of regime.

2. The electric field in a waveguide is complex in nature. However, since the purpose of this paper is just qualitative estimates, in place of real waveguide modes we will consider, as in [3], a plane wave according to the equation

$$\frac{d^2E}{dx^2} + k^2E = 0, \quad k^2 = \frac{\omega^2}{c_0^2}\left[\varepsilon_0 + i\frac{4\pi\sigma(T)}{\omega}\right], \tag{2.1}$$

where E is the electric field intensity, ε_0 is the real part of the dielectric permittivity, which is considered independent of the temperature for simplicity, and σ is the specific conductivity of the dielectric.

The heat-conduction equation describing one-dimensional stationary melting wave propagation over a waveguide without taking account of secondary heat losses has the form

$$\frac{d}{dx}\left(\lambda\frac{dT}{dx}\right) - c\rho v\frac{dT}{dx} + \frac{1}{2}\sigma(T)|E|^2 = 0, \tag{2.2}$$

where x is the coordinate, T is the temperature, λ, c, ρ is the heat conduction, specific heat, and density of the dielectric, and v is the wave velocity.

The boundary conditions for system (2.1) and (2.2) are

$$x \to -\infty,\ T = T_0,\ E = E_0\, e^{ikx} + B\, e^{-ikx},$$
$$x \to +\infty,\ dT/dx = 0,\ E = 0,$$

E_0 is the given amplitude of the incident electromagnetic wave at the waveguide input, and B is the unknown amplitude of the reflected wave.

Therefore, there is a self-consistent problem: according to (2.2) the temperature profile in the thermal wave depends on the electric field distribution, which is determined, in turn, by the temperature distribution (2.1).

3. System (2.1), (2.2) does not allow an exact analytical solution. To construct the approximate solution, the widely known method from combustion theory is used, of "cutting off" the heat liberation function in the heat-conduction equation [5]. Because of the exponential temperature dependence of the conductivity of a solid dielectric, the heat liberation power therein drops radically with the diminution in temperature. We shall consider all the heat in the solid phase to be liberated just within the characteristic temperature range $T_b < T < T_l$ ($T_b = T_l - T_l^2/\Delta$, where Δ is the width of the dielectric forbidden band, and T_l is the melting point). Because of the skin effect the heat in the melt is liberated in a narrow surface layer of width δ. A constant temperature T_m is maintained in the rest of the melt (since there is neither heat liberation nor heat loss).

In conformity with the above, the following domains can be separated out (Fig. 1) in the dielectric:

$x < 0$, $T < T_b$ is the heating zone 1;

$0 < x < l$, $T_b < T < T_l$ is the heat liberation zone into the solid phase 2;

$l < x < l + \delta$, $T_l < T < T_m$ is the heat liberation zone into the melt 3;

$x > l + \delta$, $T = T_m$ is the zone without heat liberation and heat loss 4.

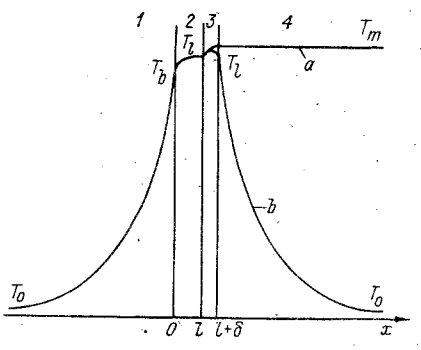

Fig. 1

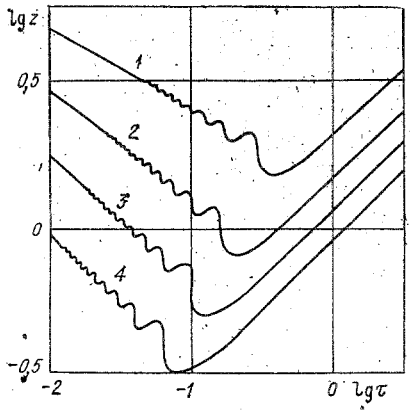

Fig. 2

The source functions and λ in (2.2) within the limits of each zone are replaced by their mean values (for the given zone). The boundary conditions are

$$x \to -\infty,\ T = T_0,\ x = 0,\ T = T_b,\ q_1 = q_2,$$
$$x = l,\ T = T_l,\ q_3 = q_2 + \rho v L,\ x = l + \delta,\ T = T_m,\ dT/dx = 0, \tag{3.1}$$

q_j is the heat flux through unit areas in the j-th zone, L is the melting heat of the dielectric. Solving the piecewise-linear system (2.2) with the boundary conditions (3.1), the temperature profile (Fig. 1, curve a) and the distribution of the heat flux $q_j = \lambda_j(dT/dx)$.

Under the condition

$$q_2(x = l) = 0 \tag{3.2}$$

all the heat being liberated in the melt will go into melting the substance while heating of the solid phase occurs because of the intrinsic heat liberation source Q_s. Condition (3.2) determines the critical value of the power being delivered to the waveguide input from the microwave generator since melt crystallization occurs as it is reduced further. The relationships

$$l = 2\gamma\chi_s v^{-1},\ v = (2\gamma\chi_s Q_s/c\rho)^{1/2}(T_l - T_0)^{-1/2},\ Q\delta = \rho v L \tag{3.3}$$

are obtained from (3.1) and (3.2), where $\gamma = (T_l^2/\Delta)(T_l - T_0)^{-1}$, χ_s is the thermal diffusivity of the solid dielectric, Q is the power of heat liberation per unit volume, and the subscript s denotes that the quantity belongs to the solid phase. System (3.3) of three equations does not determine the four unknowns v, l, Q_s, and Q. The missing fourth relationship can be obtained from the "electrical" equation (2.1) by solving it in conformity with the melting wave model taken for a constant value of σ within the limits of each zone. The solution in the j-th zone has the form

$$E_j = A_j e^{ik_j x} + B_j e^{-ik_j x},$$

where A_j and B_j are complex amplitudes of the incident and reflected waves that should be found from the boundary conditions. Considering the incident wave amplitude at the waveguide input to be the given quantity $A_1 = E_0$ and setting the coefficient of reflection from the melt equal to one (only for the approximate computation of the field in the solid phase), we write the continuity condition for the electrical and magnetic fields on the boundary of zones 1 and 2 in the form

$$E_0 + B_1 = A_2[1 - \exp(2ik_2 l)];\ k_1(E_0 - B_1) = k_2 A_2[1 + \exp(2ik_2 l)],$$

from which

$$B_1 = \frac{k_1[1 - \exp(2ik_2 l)] - k_2[1 + \exp(2ik_2 l)]}{k_1[1 - \exp(2ik_2 l)] + k_2[1 + \exp(2ik_2 l)]} E_0; \tag{3.4}$$

$$A_2 = \frac{2k_1}{k_1[1 - \exp(2ik_2 l)] + k_2[1 + \exp(2ik_2 l)]} E_0. \tag{3.5}$$

The Poynting vector for the incident electromagnetic wave in the j-th zone is (S_{j0}, 0, 0)

$$S_{j0} = (c_0^2/8\pi\omega)\,\mathrm{Re}\,k_j\,|A_j \exp(ik_j x)|^2. \tag{3.6}$$

Heat flux of density

$$S_2 = (1 - R)S_{10} = Q_s l + Q\delta \tag{3.7}$$

goes into zone 2 and

$$S_3 = (1 - R_3)S_{20}|_{x=l} = Q\delta \tag{3.8}$$

into zone 3, where R is the reflection coefficient, and R_3 is the reflection coefficient from zone 3. The ratio

$$Q_s/Q = \delta l^{-1}[(1 - R)(1 - R_3)^{-1}(S_{10}/S_{20}|_{x=l}) - 1] \tag{3.9}$$

is obtained from (3.7) and (3.8). The reflection coefficient

$$R = |B_1/E_0|^2 \tag{3.10}$$

and R_3 can be written in the form

$$R_3 = |(k_3 - k_2)/(k_3 + k_2)|^2$$

(see [6], say). Expanding this last expression in a power series in the small quantity $(\sigma_S/\sigma)^{1/2}$ and limiting ourselves to linear terms, we obtain R_3 in the form

$$R_3 = 1 - (a + b)(2\varepsilon_0\omega/\pi\sigma)^{1/2}, \tag{3.11}$$

where $a = \mathrm{Re}\sqrt{1 + i(4\pi\sigma_s/\varepsilon_0\omega)}$, $b = \mathrm{Im}\sqrt{1 + i(4\pi\sigma_s/\varepsilon_0\omega)}$. Taking account of (3.6), (3.10), and (3.11), the expression (3.9) becomes

$$Q_s/Q = \delta l^{-1}\left[(\pi\sigma/2\varepsilon_0\omega)^{1/2}a^{-1}(a + b)^{-1}\left(E_0^2 - |B_1|^2\right)|A_2\exp(ik_2 l)|^{-2} - 1\right]. \tag{3.12}$$

This is indeed the relationship closing system (3.3). There follows from (3.3)

$$Q_s/Q = (\delta c/lL)(T_l - T_0). \tag{3.13}$$

Eliminating the ratio Q_S/Q from (3.12) and (3.13), an equation can be obtained in l, the width of zone 2:

$$E_0^2 - |B_1|^2 = a(a + b)(2\varepsilon_0\omega/\pi\sigma)^{1/2}[1 + (c/L)(T_l - T_0)]|A_2\exp(ik_2 l)|^2. \tag{3.14}$$

The expressions for the complex amplitudes B_1 and A_2 are given by (3.4) and (3.5). Computing the magnitude of l from (3.14), values of v, Q_S, and Q can be determined by means of (3.3). After calculating the moduli of the complex quantities and reducing similar terms, (3.14) can be rewritten in the dimensionless form

$$\begin{gathered}\tau^{1/2}(a - b)[\mathrm{sh}(b\tau^{-1}z) - (b/a)\sin(a\tau^{-1}z)] = N,\\ a = \mathrm{Re}\sqrt{1 + i\tau},\ b = \mathrm{Im}\sqrt{1 + t\tau},\end{gathered} \tag{3.15}$$

where $z = 8\pi\sigma_S l\varepsilon_0^{-1/2}c_0^{-1}$ is the dimensionless thickness of zone 2, $\tau = 4\pi\sigma_S(\varepsilon_0\omega)^{-1}$, $N = (2\sigma_S/\sigma)^{1/2}[1 + (c/L)(T_l - T_0)]$. The quantity z^{-1} can be considered as the dimensionless velocity of the melting wave since $z = 16\pi\gamma\sigma_{S\chi S}\varepsilon_0^{-1/2}(c_0 v)^{-1}$ according to (3.3). The dependence of z on τ computed numerically from (3.15) is shown in Fig. 2 for N = 0.5, 0.2, 0.1, 0.05 (curves 1-4, respectively). This is substantially the dependence of the critical thickness of zone 2 (or the minimal velocity of the melting wave) on the field frequency for different materials (large N correspond to transition metal oxides, and low N to semiconductors). It is nonmonotonic in nature: as the frequency increases, the wave velocity passes through a maximum. By using (3.4), (3.10), and (3.15), the dependence of the reflection coefficient R on τ and N can be computed (Fig. 3, N = 0.05, 0.1, 0.2, 0.5, curves 1-4, respectively).

As the frequency increases, the reflection coefficient diminishes (therefore the efficiency of the energy contribution increases). In the wavelength range comparable to the thickness of zone 2, oscillations in the reflection coefficient are observed because of interference phenomena. The wave velocity in this frequency range also oscillates (see Fig. 2). Interference oscillations of the absorptivity of metal–oxide systems for laser heating of metals in an oxidative medium are described in [7].

Knowing the frequency dependences of the velocity (see Fig. 2), and the reflection coefficient (see Fig. 3), the frequency dependence of the minimal energy flux delivered to the waveguide input from the microwave generator can be determined. According to (3.3) and (3.7), the density of this flux has the following form in dimensionless variables

$$P = [(1 - R)z]^{-1}, \tag{3.16}$$

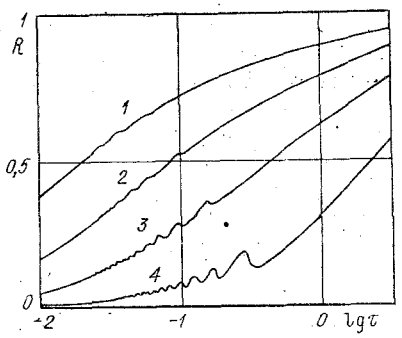

Fig. 3

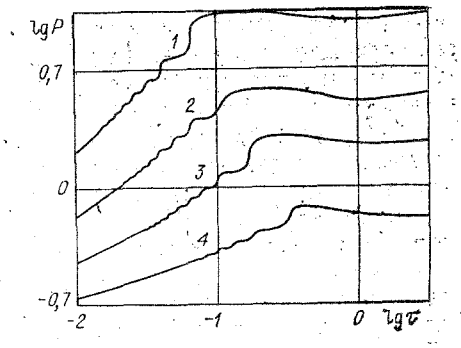

Fig. 4

where

$$P = (c_0\varepsilon_0^{1/2}/16\pi\gamma\sigma_s\lambda_s)(T_l - T_0 + Lc^{-1})^{-1}S_{10}.$$

The series of curves $P = P(\tau, N)$ is displayed in Fig. 4, where the lines 1-4 correspond to $N = 0.05, 0.1, 0.2, 0.5$. If the value of the delivered power flux P_0 is below the appropriate curve, the melt vanishes. Formulas from [3] become applicable here to describe the thermal wave. As numerical estimates show, the thickness of zone 2 increases upon going over to $P_0 < P(\tau, N)$, while the reflection coefficient drops to practically zero. The wave velocity grows, which is related to both the diminution in R and to the absence of heat expenditure in the phase transition. The zone 2 in which all the field energy is absorbed, "runs away" from zone 3 and the melt freezes. This phenomenon is similar to the passage from the "control" regime to "separation" in the theory of multizone combustion [8].

4. Adiabatic melting wave propagation over a dielectric waveguide was considered above. The influence of the second heat losses on the fundamental process characteristics (wave velocity, minimal energy expenditures, maximal melt temperature) can be taken into account if the term $[-4\mathrm{Bid}^{-1}\lambda(T - T_0)]$ is inserted in the left side of the heat-conduction equation (2.2). As mentioned above, the melt domain becomes bounded in the nonadiabatic case. Its width depends on the intensity of the heat elimination, i.e., on the Biot criterion Bi. Let us limit ourselves to a computation of the Bi for which this width will agree with the width of the skin layer δ. The structure of such a melting wave is shown in Fig. 1 (curve b). Heat elimination from the waveguide surface occurs mainly in zones 1 and 4 since their width is much greater than the widths of zone 2 and 3. Consequently, the secondary heat elimination cannot be taken into account in writing the heat-conduction equation in zones 2 and 3. The boundary conditions for the first three zones remain as before. For zone 4 they are

$$x = l + \delta,\ T = T_l,\ q_3 - q_4 = \rho v L;\ x \to +\infty,\ T = T_0.$$

Calculations result in an equation for the width of zone 2 that agrees with (3.15); however, the parameter N becomes

$$N = (\sigma_s/\sigma)^{1/2}[4 + (c/L)(T_l - T_0)].$$

The dependences $z = z(\tau, N)$ and $R = R(\tau, N)$ represented in Figs. 2 and 3 are valid even for the nonadiabatic case. The melting wave velocity is related to the width of zone 2 by the relationship

$$v = 2\gamma\chi_s l^{-1}[1 + 2Lc^{-1}(T_l - T_0)^{-1}]^{-1}.$$

The maximal temperature of the melt is

$$T_m = T_l + (Q\delta^2/8\lambda).$$

The mean heat liberation power densities in the solid phase and in the melt are

$$Q_s = 2\gamma\lambda_s l^{-2}(T_l - T_0),$$
$$Q = 2\gamma\lambda_s(l\delta)^{-1}(T_l - T_0)[1 + (c/2L)(T_l - T_0)]^{-1},$$

and the corresponding value of the Biot criterion is

$$\mathrm{Bi} = 2\gamma(d/l)^2[1 + (2c/L)(T_l - T_0)]^{-1}.$$

A formula that agrees with (3.16) is obtained for the quantity

$$P = (c_0\varepsilon_0^{1/2}/16\pi\gamma\sigma_s\lambda_s)(T_l - T_0)^{-1}[2 + (c/L)(T_l - T_0)][4 + (c/L)(T_l - T_0)]^{-1}S_{10}$$

so that the results represented in Fig. 4 retain their value.

In conclusion, it should be noted that insertion of a sharp boundary between zones 1 and 2 as well as the approximation $R_3 = 1$ will increase the reflection coefficient R. Hence, the computed value of the energy flux S_{10} should be considered an upper bound.

LITERATURE CITED

1. V. I. Aleksandrov, V. V. Osiko, et al., "New method of obtaining refractory single-crystals and melts of ceramic materials," Vestn. Akad. Nauk SSSR, No. 12 (1973).
2. A. G. Merzhanov, V. A. Raduchev, and É. N. Rumanov, "Thermal melting waves and dielectric crystallization," Dokl. Akad. Nauk SSSR, 253, No. 2 (1980).
3. Yu. P. Raizer, "High-pressure microwave discharge propagation," Zh. Eksp. Teor. Fiz., 61, No. 1 (1971).
4. I. E. Poyurovskaya, M. I. Tribel'skii, and V. I. Fisher, "On the ionization wave sustainable by powerful monochromatic radiation," Zh. Eksp. Teor. Fiz., 82, No. 6 (1982).
5. Ya. B. Zel'dovich, "On the theory of flame propagation," Zh. Fiz. Khim., 22 (1948).
6. L. D. Landau and E. M. Lifshits, Electrodynamics of Continuous Media [in Russian], Fizmatgiz, Moscow (1957).
7. F. V. Bunkin, N. A. Kirichenko, and B. S. Luk'yanchuk, "Thermochemical phenomena stimulated by laser radiation," Izv. Akad. Nauk SSSR, Ser. Fiz., 45, No. 6 (1981).
8. A. G. Merzhanov, É. N. Rumanov, and B. I. Khaikin, "Multizone combustion of condensed systems," Zh. Prikl. Mekh. Tekh. Fiz., No. 6 (1972).

MOTION OF A CURRENT-CARRYING PLASMA SHELL IN A RAREFACTION WAVE

V. S. Komel'kov, A. P. Kuznetsov, and A. S. Pleshanov

UDC 533.9.07

The paper is an extension of the research of [1, 2]. In [2] it was shown, both experimentally and theoretically, that a plasma shell generated by a coaxial accelerator can also be accelerated beyond the limits of the coaxial section. The existence of limits to such acceleration was also indicated there. It turned out that high parameters of the accelerated plasma can be obtained (at currents of order 1 MA) only when the gas filling the accelerator has a relatively low density (a number of hydrogen atoms $n \leqslant 10^{17}$ 1/cm^3). For the experiment described in [1, 2] the interelectrode space must be filled with a gas having a density an order of magnitude greater than that at which it is possible to obtain a high-temperature plasma. A conflict arises between the demands for performing the experiment and the conditions for obtaining high-parameter plasma formations. This conflict can be eliminated, in our view, if the plasma is accelerated in a rarefaction wave propagating opposite to the motion of the plasma shell. With the appropriate synchronization of the motion of the plasma and the rarefaction wave one can assure the development of a discharge and the formation of a shell in a sufficiently dense gas, while the plasma acceleration occurs, as in [2, 3], beyond the cut of the accelerator in the considerably less dense medium formed by the rarefaction wave.

The present work was devoted to a numerical investigation of the possibilities of such plasma acceleration. One of the possible schemes for it is presented in Fig. 1, where 1 is the coaxial accelerator with energy storage, 2 is the accelerator chamber, 3 is a diaphragm that opens, and 4 is the evacuated section. In such an apparatus the process develops as follows. The coaxial accelerator ejects into the accelerator chamber a plasma cluster which is formed under the action of the current flowing into the shell (Fig. 2). At a certain instant the diaphragm is opened and a rarefaction wave is formed, in which the current-carrying shell to be accelerated moves.

Statement of the Problem

We consider only the process taking place beyond the cut of the coaxial plasma accelerator. The plasma emitted from the accelerator consists of an axisymmetric shell formed by the

Moscow. Translated from Zhurnal Prikladnoi Mekhaniki i Tekhnicheskoi Fiziki, No. 1, pp. 13-18, January-February, 1985. Original article submitted October 31, 1983.

0021-8944/85/2601-0010$09.50